DISCUSSION OF THE IMPACT OF DATA CONTAMINATION ON TDWR ALGORITHM PERFORMANCE*†

Mark A. Isaminger, Benjamin G. Boorman, and Bradley A. Crowe

M.I.T. Lincoln Laboratory
Lexington, Massachusetts 02173

1. INTRODUCTION

The Federal Aviation Administration (FAA) is currently deploying Terminal Doppler Weather Radars (TDWRs) at key airports in the continental U.S. that experience high volumes of traffic and high frequencies of thunderstorm impact. The TDWR is designed to display the location and intensity of storm cells as well as the location and intensity of wind shear events in the airport vicinity. The TDWR system uses clutter filters and four data quality editing techniques: point target removal, clutter residue editing maps (CREMs), range obscuration editing, and velocity dealiasing in an attempt to reduce base data contamination prior to wind shear algorithm processing.

The performance of the wind shear detection algorithms is directly related to the quality of the base data. In particular, failures of the data quality editors can seriously degrade the wind shear detection algorithm's performance. It will be shown that these failures can lead to both undetected and false events. In addition, clutter contamination from non-meteorological sources such as birds can produce false wind shear signatures in the radar data. This paper will examine the impact of data contamination on algorithm performance at key TDWR sites where base and products data have been collected. The severity of these failures will be discussed, along with possible solutions to the most significant problems.

2. DESCRIPTION OF PROBLEMS

For this report, we analyzed base and products data from a number of TDWR sites such as Denver (DVX), Orlando (MCO), Memphis (MEM), Washington National (DCA), Dallas Love (DAL), St. Louis (STL), Oklahoma City Training Academy (OEX) and Oklahoma City Program Support Facility (PSF). From this we were able to determine a number of data quality and algorithm problems. The following is a list of the problems discussed in this report.

- Velocity dealiasing contamination,
- Out-of-trip weather,
- Clutter breakthrough,
- Data removal by clutter polygons,
- Distant clear-air returns obscuring in-trip clear-air,
- Ring of missing data due to high signal-to-noise (SNR) values in the gates used for system diagnostics,
- Radar switching into hazardous mode on reflectivity cells that do not meet the reflectivity length requirement, and
- Data contamination due to moving clutter sources such as birds or vehicles.

2.1 Velocity Dealiasing Contamination

The first problem we analyzed was the contamination of the TDWR velocity data from incorrect dealiasing. The TDWR employs a low pulse repetition frequency (PRF) tilt at the beginning of the volume scan to estimate the coverage, intensity and location of all echoes between the radar's normal unambiguous range and 460 km. Each of the tilts within the scan are assigned a PRF based on the potential obscuration. If there is little obscuration, the algorithm will employ a higher PRF (higher unambiguous velocity). If there is significant obscuration, the PRF chosen will be smaller, and hence there is also a smaller unambiguous velocity. The TDWR uses a velocity dealiasing algorithm in an attempt to correctly unfold the velocities that exceed the maximum unambiguous velocity. This is accomplished primarily by the construction of a Wind Field Model (WFM)

* This work was sponsored by the Federal Aviation Administration. The views expressed are those of the authors and do not reflect the official policy or position of the United States Government.

† Opinions, interpretations, conclusions and recommendations are those of the authors and are not necessarily endorsed by the United States Air Force.

based on the velocity data on each tilt. The following conditions have been identified as causing the WFM to be corrupted.

- Susceptibility to data contamination from noise, out–of–trip echoes or velocity dealiasing failures and
- Susceptibility to errors caused by transient outflow features such as gust fronts that do not fit the model's uniform wind field assumptions.

Based on an analysis of data collected at the previously mentioned TDWR sites, contamination from velocity dealiasing errors was one of the primary contributor's to gust front algorithm false alarms and missed events. According to Vasiloff (1993), approximately two–thirds of the gust front false alarms during the OEX testing were caused by velocity dealiasing errors. An analysis of gust front algorithm performance at MEM and DCA also showed a significant percentage of false alarms due to dealiasing failures (Klingle–Wilson et al., 1996). Our experience with the Integrated Terminal Weather System (ITWS) prototype testing at MEM and DAL showed that velocity dealiasing errors can mask the convergent signature and lead to a partial detection or a complete miss.

This type of problem was evident with a strong MEM gust front on 19 April 1996. The WFM became corrupted by a gust front which produced inbound velocities in a region of strong outbound environmental flow. The velocity errors covered a small region at first, but as these bad values were input back into the WFM, the coverage and intensity of the errors increased. Eventually they masked a large percentage of the convergent signature, making a detection virtually impossible. An example of this case is shown in Figure 1. The velocity dealiasing errors are represented by the wedge of outbound velocities located between 40 to 60 km range and 335 to 350 degrees azimuth (region is highlighted with dark polygon). This was an example of a serious algorithm failure since the wind shift associated with the front was quite significant (342 degrees and 37 knots). The velocity dealiasing errors also corrupted the wind shift estimates associated with the boundary on those scans when it was detected. While not as common, it can also negatively impact the performance of the microburst detection algorithm by masking the wind shear signature. This was evident with two hail–producing squall–lines that impacted MCO on 6 March and 25 March 1992.

2.2 Out–of–Trip Weather

The second data quality problem that hampers primarily gust front detection algorithm performance is obscuration from echoes beyond the unambiguous range of the radar. As with velocity dealiasing errors, this problem can also cause false events and misses. As discussed previously, the TDWR employs a low PRF tilt to determine how much obscuration there is at the beginning of the hazardous or monitor scan sequence. Each of the tilts are assigned the highest PRF possible as long as the obscuration does not exceed a pre–defined maximum obscuration threshold. The algorithm assigns PRFs based on location priority, e.g., AREas Noted for Attention (ARENAS), hazardous sector and full domain. In the case of large storm systems, the amount of obscuration overwhelms the algorithm and there is a significant amount of range obscured data within the airport sector. The algorithm attempts to edit these data, but the performance is degraded because the obscuration map is limited by both spatial and temporal constraints. The gust front signature can be masked if it propagates through the data void/contamination region.

An example of this is shown in the 08 July 1996 case from MEM (Figure 2). A fairly long gust front feature is evident in the velocity data to the north and northeast of the radar at a range of 30 to 80 km (represented by the transition from light grey to dark grey). The large data void region between 000 and 045 degrees azimuth is due to range obscuration editing. The gust front algorithm is able to detect only the western extent of the front (curved white line located at 30 km and 345 degrees) due to the data void. Thus, a large percentage of this feature went undetected.

2.3 Clutter Breakthrough

In order to reduce base data contamination from stationary clutter targets, the TDWR employs a high pass filter which reduces the signal strength of echoes near 0 m/s by approximately 50 dB. The CREMs then flag data as invalid in range gates where the received echo power does not exceed the clutter residue level by less than a statistically significant margin. If there is significant variability in the clutter residue level, the resulting clutter breakthrough could produce false wind shear alarms (Merritt et al., 1989). This would especially be the case if the average variability exceeds the CREM breakthrough parameter.

During optimization trips to DAL and DCA, clear–air/clutter data were collected with and without the clutter filters on each radar channel at the lowest site specific elevation angle required for microburst detection. The data set that was collected provided the opportunity to analyze the scan to scan clutter variability between the reflectivity (DZ) and SNR data using a statistical program that allows for a comparison between multiple sets of input data. In order to ensure a higher percentage of clutter targets, the range extent was limited to within 20 km of the radar. Since we did not exclude the low reflectivity clear–air returns, they would also contribute some to the variability discussed here.

Tables 1A through1D present data pertaining to the clutter variability for SNR and DZ data at DAL and DCA. Here, clutter variability is defined as the root mean squared (RMS) scan–to–scan fluctuation in clutter (or clutter residue) power in an individual range gate. The ensemble average of this quantity is estimated by averaging the single range gate RMS measurements over all range gates within 20 km of the radar. On average, the clutter variability at DAL was similar to the results from DCA. In terms of the comparison between radar channels, there was less than 0.5 dB difference for both sites. This was not the case when we compared the variability between the filtered and unfiltered data. In general, the filters had 2 to 3 dB more variability. An examination of the spatial distribution of the variability indicated it was randomly distributed across the region that was analyzed. There were some pockets of higher variability that could have been associated with vehicular traffic on major highways or highway intersections. It was also important to note that the clutter breakthrough parameter used at DAL was 8 dB. According to these results, it would not account for the average variability at this site. The DAL site would require a slightly higher breakthrough parameter in order to be more effective at reducing clutter breakthrough.

Next, we examined the clutter variability between DZ and SNR to determine if they were similar. In general, the SNR variability for DAL was between 1 and 3 dB for all of the categories. By comparison, the DZ varied from 4.5 to 9.5 dB at this site for the same categories, while there was more variability (several dB) with the filtered data for both DZ and SNR. The results were similar for DCA; e.g., 1 to 3 dB variability for SNR and 3 to 10 for DZ. At DCA, a comparison of the filtered and unfiltered data showed only a slight difference, e.g., generally less than 1 dB. The higher variability with the filters at DAL was probably due to a higher percentage of moving versus stationary clutter targets.

The results of this analysis clearly showed that there was 2 to 3 times more variability in the DZ data versus SNR. This was consistent for all of the variables that were analyzed, e.g., filter, no filter; intra–channel, inter–channel; STC and no STC. This was difficult to understand since the DZ values were based on SNR and thus should be comparable. We have proposed the following two hypotheses as possible reasons for this discrepancy.

- The point target filter is applied to the SNR field and not DZ or
- There is an error in the conversion from SNR to DZ.

2.4 Clutter Map Polygon Problems

The TDWR uses CREMs on the lowest elevation tilts generated from data collected under clear–air conditions to map out those areas that contain stationary clutter returns. The maps were constructed by averaging the gate–to–gate data collected from at least 20 tilts. Based on an analysis by Hynek (1990), the clutter maps performed better using the median value since this technique removed outliers due to airplanes or vehicles. Hynek also found that the maps were not very effective at flagging moving clutter such as vehicular traffic along highways. In these areas, the operator can install clutter polygons in an attempt to remove the breakthrough. One limitation of the polygons is that they allow only a single reflectivity value to apply to all breakthrough points within the polygon. At DAL, the clutter breakthrough around the airport was so severe that it required numerous high–reflectivity polygons to reduce the data contamination. Since the clutter polygons were so aggressive, they also removed data associated with weather echoes.

On 14 June 1996, there was a microburst near the ARENAS at DAL whose velocity differential was significantly underestimated on the 0.1 degree tilts due to this problem. This problem was not apparent at 0.3 degrees because the clutter breakthrough did not require any polygons on this tilt. As shown in TABLE 2, the loss values for this event during real–time using the 28 November 1995 polygons were typically reported as 25–40 knots. Due to this problem, we decided the polygons at DAL were too aggressive and needed to be regenerated. This was accomplished by the TDWR Program Support Facility (PSF) on 27 June 1996. Once the less aggressive polygons were installed, the algorithm loss values varied from 40 to 65 knots, which was a more accurate representation of the hazard associated with this event. If there are still detection problems in the polygon regions at this site, we will recommend the minimum surface elevation for microburst detection be raised from 0.1 to 0.2 degrees to reduce the clutter residue.

2.5 Distant Clear–air Problems

Another problem identified deals with the removal of in–trip clear–air returns based on distant clear–air returns. We have seen clear–air data as high as 10 dBz removed due to this problem. It is an issue for low reflectivity features such as gust fronts and dry microbursts since the returns from these events are typically less than 10 dBz. Thus, this problem could impact the ability of the system to detect these low reflectivity wind shear features.

The calculation of DZ in the TDWR system follows a $1/r^2$ relationship which causes the reflectivity estimate for a constant power return (such as system noise) to be increased with increasing distance from the radar. Since the low PRF tilt is designed to detect signals out to 460 km, this can result in the system noise exceeding the in–trip weather values, especially if there are few or no clear–air scatterers in the first–trip region. If the difference is greater than the distant weather threshold, which is 5 dB, the out–of–trip returns are assumed to be weather. In this case, the range obscuration algorithm removes the in–trip signal.

This problem was first observed on 17 June 1994 in the MEM data. Since then, it has also been documented on a sporadic basis at several other TDWR sites such as MCO and DAL. We proposed the following factors that could account for it.

- The obscuration algorithm is using DZ instead of SNR to compute distant weather obscuration,
- Incorrect or insufficient parameter settings,
- A discrepancy in the calculation of SNR between the low and normal PRF tilts, or
- Attenuation of the clear–air returns in the first trip by the clutter filters which would allow the out–of–trip clear–air returns to obscure the in–trip returns in regions with near zero Doppler velocities.

An SNR image from 182129 UT on 17 June 1994 (Figure 3) shows two large areas of data removed to the northwest and southeast of the radar. In sharp contrast, there was very little data removed in the clear–air returns to the northeast and southwest. The SNR returns from the low PRF tilt at 182055 UT (Figure 4) showed several features that were pertinent to this analysis. First, the SNR in every gate was above the minimum detectable signal, e.g., 0.5 dB. In fact, the SNR of the clear–air returns that were removed were as high as 18 dB, while those returns greater than 18 generally went unedited. A reflectivity image from the Millington NEXRAD (not shown) indicated that there were a few isolated cells located beyond the TDWR's unambiguous range to the northwest and southeast. These cells, however, do not encompass enough area to account for all of the edited regions observed in the TDWR data at 182129. Interestingly, though, there were clear–air returns of 10 to 15 dBz, in the out–of–trip areas that would correlate to the range obscured regions in the first trip. So, it is possible in this case that the algorithm removed the in–trip data based on clear air as well as distant storms.

The next issue concerns how the SNR of the out–of–trip clear–air is different from the in–trip returns. Understanding how the clear–air returns could be edited required a gate–by–gate comparison of the SNR between the low PRF and second dual–PRF tilts. To determine if obscuration was the source of the problem, we analyzed data between 35 and 45 km range along the 290 degree radial. This was one of the radials where clear–air returns were removed. Based on a PRF of 1193, the maximum unambiguous range for this tilt was 125.7 km. We then calculated the ranges at which distant weather could potentially obscure in–trip signals between 35 and 45 km. These ranges were 160 to 170, 286 to 296 and 412 to 422 km. By examining the SNR returns from the areas of potential obscuration we noticed that the recorded values were not sufficient to obscure the in–trip returns. In fact, most of the in–trip gates generally had higher returns than their corresponding out–of–trip gates. Finally, we noted that the SNR returns on the low PRF and dual–PRF tilts were similar in this case (see Figures 3 and 4). This would rule out any possibility of a miscalculation of SNR between these two tilts, at least in the recorded base data.

Next, we explore the possibility that the range obscuration algorithm used DZ instead of SNR to compute distant weather obscuration. We compared the gate–to–gate DZ values between the in–trip region and the corresponding out–of–trip areas (not shown), and there was generally a difference of greater than 10 dB. This would be sufficient for the out–of–trip clear air to obscure the in–trip clear air. However, when we examined the algorithm code, we could not confirm it was using DZ.

Finally, we hypothesize that the clutter suppression filters could have reduced the in–trip clear air sufficiently in low velocity gates to allow the distant weather criteria to be satisfied. The filters were applied only at ranges less than 90 km from the radar. Thus, returns at greater ranges would not be attenuated by the filters. An examination of the velocity values along the 290 degree radial between 35 and 45 km showed that all of the values were less than 1.5 m/s. This was certainly within the notch of the high–pass filter. Therefore, for those radials that contained low reflectivities and low velocities, such as along or near the zero Doppler line, the unfiltered out–of–trip clear air could have obscured the filtered in–trip clear air. This would explain some of the editing that occurred on 17 June 1994. Whether this is the only problem or not is still open to discussion.

What steps could be taken to eliminate this problem in the future?

- Change the filtering scheme so the high pass filter is applied to every gate on the low PRF tilt. This could involve changes to the hardware, or
- Change the range obscuration and distant weather thresholds so distant clear–air returns will not obscure the in–trip clear air. A study will be conducted to determine appropriate obscuration thresholds based on the filter attenuation factor and the fact that the in–trip signal is at least 6 dB higher due to beam filling losses in the distant returns.

2.6 Ring of Missing Data

Another problem identified was a ring of missing data in the low signal returns surrounding the radar site at DVX. This problem was apparent on both the low PRF and second dual–PRF tilts. It was definitely related to low SNR values since there were higher clutter/second–trip returns embedded within the ring. The problem was caused by the clutter breakthrough parameter which was applied to all of the range cells within the first–trip region instead of just the clutter gates. Since it was typically a low signal problem and did not impact the performance of the wind shear detection algorithms, a decision was made not to correct the implementation error.

Another manifestation of this problem is a ring of missing data over several range gates at variable distances in the base data. An example of this problem from OEX is shown in Table 3. There are two gates of missing data centered at 17.17 km range. We believe the source of this problem is the number of valid range gates used for processing the low PRF data. An examination of the low PRF data revealed that there are 1984 range gates. According to the TDWR specification, there are only 1981 valid range gates since the last three gates are used for digital signal processor (DSP) diagnostics. An examination of the SNR values in the last few gates showed a ring of high values. When this data was folded back into the first trip region, the range obscuration algorithm assumed it was weather and set the Compressed Condition flag to valid (CCV). This resulted in the removal of the in–trip returns whenever the obscuration threshold was exceeded.

Since the three gates beyond 1981 are used for diagnostics, they should not be processed by any of the TDWR algorithms. We suspect that the obscuration algorithm is reading the "range samples per dwell" message in the header and not the "final range sample" number. This problem could affect the wind shear detection algorithm performance by removing data associated with a gust front or by removing data within the outflow region of a wind shear or microburst. In fact, we have already documented a case from MCO where the ring of missing data caused three wind shear events within the ARENAS to be missed. There were several other events whose spatial extent was underestimated due to the data void. The simplest solution to this problem would be for the range obscuration algorithm to ignore the data in the last three range gates of the low PRF tilt.

2.7 Hazardous Mode Switch Problem

The TDWR system uses an algorithm based on the DZ field to decide when to switch from monitor to hazardous mode. In order for a DZ segment to be valid it must contain values of at least 30 dBz over a distance of at least 13 range gates above a minimum altitude of 2 km AGL. The entire reflectivity segment must also be within the hazardous sector azimuth limits and 45 km of the Airport Reference Point (ARP). We have documented numerous examples of incorrect scan mode switching at every site where data was collected. For this report, we will show one case from MEM to illustrate the problem. The case in question occurred on 24 June 1996 at 174625 UT. The last monitor tilt prior to the switch to hazardous mode was 6.1 degrees. The data from this tilt was examined and there was only one weak reflectivity feature located within the sector at a range of approximately 21 km from the radar. An examination of the DZ (Table 4A) and SNR (Table 4B) data showed that the reflectivity length requirement was exceeded only on the SNR data. Thus, we hypothesized that the algorithm was using SNR instead of DZ. The code was examined and there were no obvious errors. Thus, the cause of this problem is still being investigated.

2.8 Moving Clutter

One of the most significant problems in terms of producing false gust front and microburst events was caused by moving clutter sources such as birds. According to Isaminger (1995), this problem was especially troublesome at sunrise and sunset when near–surface bird activity peaked. At those sites, such as MEM, where the roosting locales were near an ARENA, these "birdbursts" caused false wind shear and microburst alerts whenever there were weather echoes nearby. In the case of birds, the reflectivity signature did not encompass enough vertical extent in order for a storm cell to be produced. Thus, if there were no weather cells in the vicinity of the birdburst, the microburst algorithm invalidated any possible false detections. Once the birds had taken off, they aligned themselves in a manner that resembled a front, which then tricked the gust front algorithm into producing false events. The Houston Intercontinental (IAH), STL and MEM systems have all experienced false detections due to this phenomenon. In the case of the current gust front algorithm, there is no parameter that can be adjusted to eliminate these false events.

3. CONCLUSIONS

This report showed that the TDWR system as currently fielded still has a number of data quality problems that require attention if wind shear detection algorithm performance is to be optimal. The most significant problems were contamination from velocity dealiasing errors, range folding/editing and birds. Modifications to the velocity dealiasing algorithm parameters should be tested to determine if they can improve the performance. If this does not correct the problem, then we should investigate if the algorithm would work better without the WFM since it was the source of the majority of the errors. Another problem identified that should be corrected was scan switching on cells below the minimum length threshold. This problem caused the system to spend excessive time in hazardous mode on reflectivity features that were not capable of producing wind shear. We will investigate whether changing the significant reflectivity thresholds slightly can mitigate the problem somewhat. Finally, the editing of weather based on the gates used for DSP diagnostics should be corrected since it can negatively impact the performance of both the gust front and microburst detection algorithms. We should be able to solve the distant clear–air editing problem fairly simply by changing the thresholds to be less sensitive to low reflectivity returns indicative of clear air. The bird and clutter variability problems need further investigation to determine the most appropriate course of action.

4. REFERENCES

Hynek, D.P., "Use of Clutter Residue Editing Maps During the Denver 1988 Terminal Doppler Weather Radar (TDWR) Tests," MIT Lincoln Laboratory, Lexington, MA, Project Report ATC–169, 1990.

Isaminger, M.A., "Techniques for Discriminating Biological Targets from Wind Shear Events Using Doppler Radar and Atmospheric Soundings," 27TH Conference on Radar Meteorology, Vail, CO, pp. 659–662, 1995.

Klingle–Wilson, D., M. Isaminger and C. Keohan, "Report on Product Performance for the Terminal Doppler Weather Radars at Washington National Airport, and Memphis and Orlando International Airports," MIT Lincoln Laboratory, Lexington, MA, Project Report ATC–246, 1996 (publication pending).

Merritt, M.W., D. Klingle–Wilson and S.D. Campbell, "Wind Shear Detection with Pencil–Beam Radars," *Lincoln Laboratory Journal,* Vol. 2, No. 3, MIT Lincoln Laboratory, Lexington, MA, p. 483, 1989.

Vasiloff, S., "Terminal Doppler Weather Radar (TDWR) Operational Test and Evaluation: Final Report on Weather–Detection Performance," National Severe Storms Laboratory, Techniques Development Branch, Storm–Scale Research and Applications Division, Norman, Oklahoma, 1993.

5. ACKNOWLEDGEMENTS

We thank the following individuals who contributed to the completion of this report. The data presented in Table 2 was compiled by Chris Keohan and Paul Biron of the TDWR PSF. They also were responsible for installing the new clutter maps and polygons at DAL and were instrumental in identifying the cause of the data removal at DVX. The manuscript was thoroughly reviewed by Dr. Mark Weber and Leslie Mahn. Their comments were crucial in making the final report more cohesive.

TABLE 1A.
CLUTTER/CLEAR–AIR VARIABILITY
FOR DAL SNR DATA

FILTER	CHAN-NEL	STC (0–10 km)	NO STC (10–20 km)
N	BOTH	1.187	1.181
N	A	1.107	0.941
N	B	1.097	0.934
Y	BOTH	2.901	2.690
Y	A	2.671	2.355
Y	B	2.772	2.365

TABLE 1B.
CLUTTER/CLEAR–AIR VARIABILITY
FOR DAL DZ DATA

FILTER	CHAN-NEL	STC (0–10 km)	NO STC (10–20 km)
N	BOTH	6.424	5.479
N	A	6.135	4.937
N	B	5.734	4.634
Y	BOTH	9.592	7.361
Y	A	8.389	5.341
Y	B	8.598	5.241

TABLE 1C.
CLUTTER/CLEAR–AIR VARIABILITY
FOR DCA SNR DATA

FILTER	CHAN-NEL	STC (0–10 km)	NO STC (10–20 km)
Y	BOTH	2.434	2.300
Y	A	2.073	1.659
Y	B	2.092	1.721
N	BOTH	1.578	1.412
N	A	1.339	1.055
N	B	1.371	1.148

TABLE 1D.
CLUTTER/CLEAR-AIR VARIABILITY
FOR DCA DZ DATA

FILTER	CHAN-NEL	STC (0–10 km)	NO STC (10–20 km)
Y	BOTH	9.959	6.470
Y	A	7.930	3.845
Y	B	7.931	3.807
N	BOTH	8.267	5.552
N	A	6.666	3.692
N	B	6.819	3.869

TABLE 3.
RING OF MISSING DATA FROM
OEX ON 8 MAY 1993

Az	15.38		15.68		15.98		16.27		16.58		16.88		17.17		17.48	
016.0	31	34	33	31	36	36	34	33	31	28	25	25	.	.	26	29
015.0	38	41	36	36	33	35	37	33	27	22	21	23	.	.	23	28
014.0	28	33	34	32	32	30	34	28	24	23	21	21	.	.	25	26
013.0	25	25	29	26	29	31	27	24	16	25	26	24	.	.	26	25
012.0	23	26	22	22	21	22	25	21	27	27	25	24	.	.	24	24
011.0	21	23	20	26	24	23	23	27	26	26	27	26	.	.	31	30
010.0	22	19	19	26	19	21	26	25	23	26	31	30	.	.	28	36
009.0	21	19	22	18	20	22	25	24	27	25	31	30	.	.	35	30
008.0	13	12	22	23	23	22	24	26	25	25	24	27	.	.	33	31
007.0	.	.	19	21	20	23	26	22	21	23	23	28	.	.	28	30
006.0	.	.	21	22	26	22	.	22	20	21	21	25	.	.	23	21
005.0	.	21	23	30	33	26	28	29	25	28	24	28	.	.	24	24
004.0	.	.	33	32	32	28	30	30	33	32	30	32	.	.	27	25
003.0	28	34	33	35	32	31	30	33	31	33	32	29	.	.	30	31
002.0	33	33	34	40	38	35	33	34	31	30	30	30	.	.	30	31
001.0	31	39	38	40	35	32	34	33	32	30	29	28	.	.	29	27

TABLE 2.
COMPARISON OF MICROBURST
ALGORITHM LOSS VALUES WITH CREMs
GENERATED ON 112895 AND 062796.

TIME (UT)	TILT (DEG)	DV (111495 CREMs)	DV (062796 CREMs)
213320	0.1	20.6	30.9
213508	0.1	30.9	33.4
213608	0.1	20.6	23.1
213706	0.1	20.6	23.1
213802	0.1	15.4	30.9
213950	0.1	12.9	36.0
214050	0.1	12.9	33.4
214148	0.1	12.9	28.3
214244	0.1	12.9	20.6

TABLE 4A.
DZ DATA FROM MEM ON 24 JUNE 1996

Az	20.17		20.48		20.77		21.08		21.38		21.67		21.98		22.27
358.5	10	7	–5	4	11	23	28	24	25	19	13	15	14	16	11
359.5	17	17	21	25	33	34	30	30	26	23	17	20	20	22	16
000.5	8	11	21	23	23	33	26	24	28	28	29	23	23	20	18
001.5	–1	9	18	17	19	18	18	19	29	30	28	24	24	24	20
002.5	–12	–1	5	10	10	14	18	22	28	33	28	29	29	25	22

TABLE 4B.
SNR DATA FROM MEM ON 24 JUNE 1996

Az	20.17		20.48		20.77		21.08		21.38		21.67		21.98		22.27	
358.5	30	27	16	24	31	43	48	44	45	39	32	34	33	36	30	28
359.5	37	37	41	46	53	54	50	50	45	43	37	39	40	41	35	32
000.5	29	31	41	43	43	53	46	44	47	48	48	43	42	40	38	40
001.5	19	29	38	38	39	38	38	39	49	50	48	43	44	43	39	38
002.5	9	20	25	31	30	34	38	42	48	53	48	48	48	45	41	36

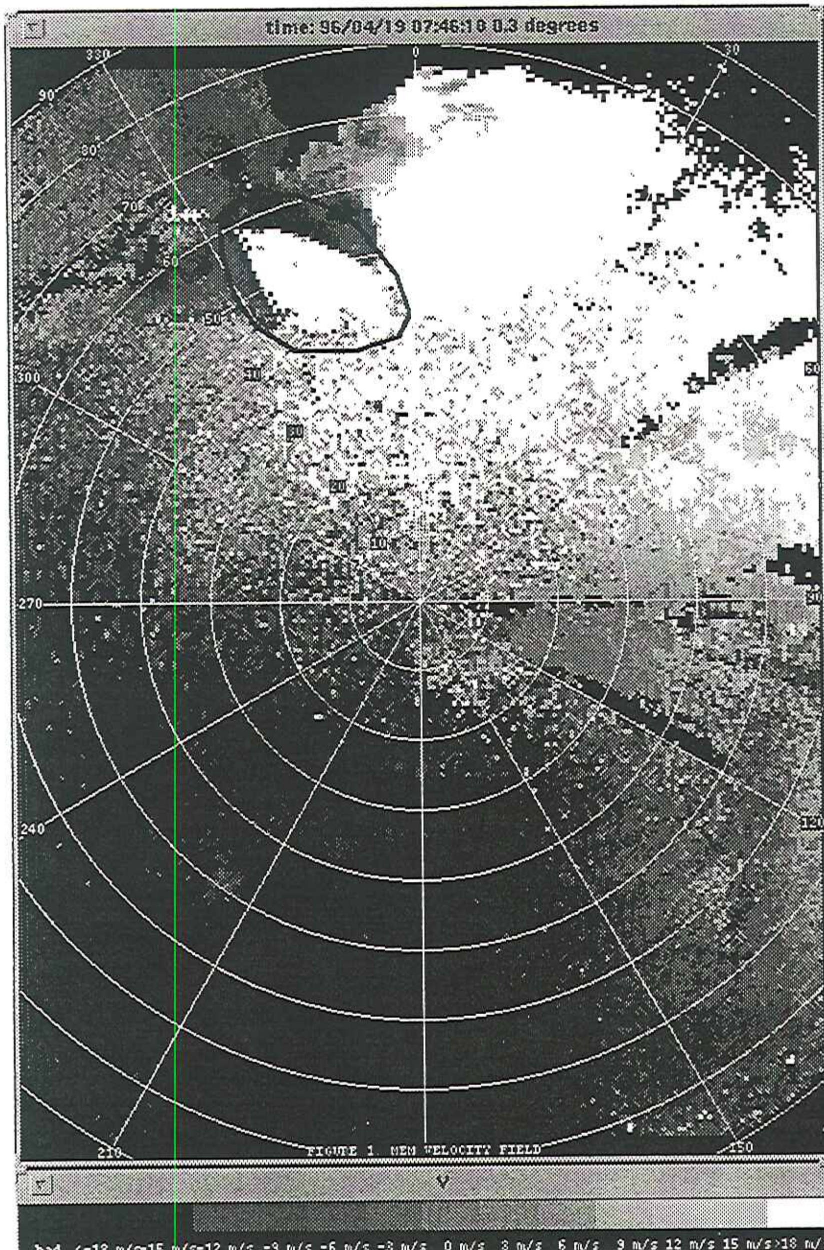

Figure 1. MEM TDWR velocity field showing gust front algorithm performance degradation due to velocity dealiasing errors on 19 April 1996.

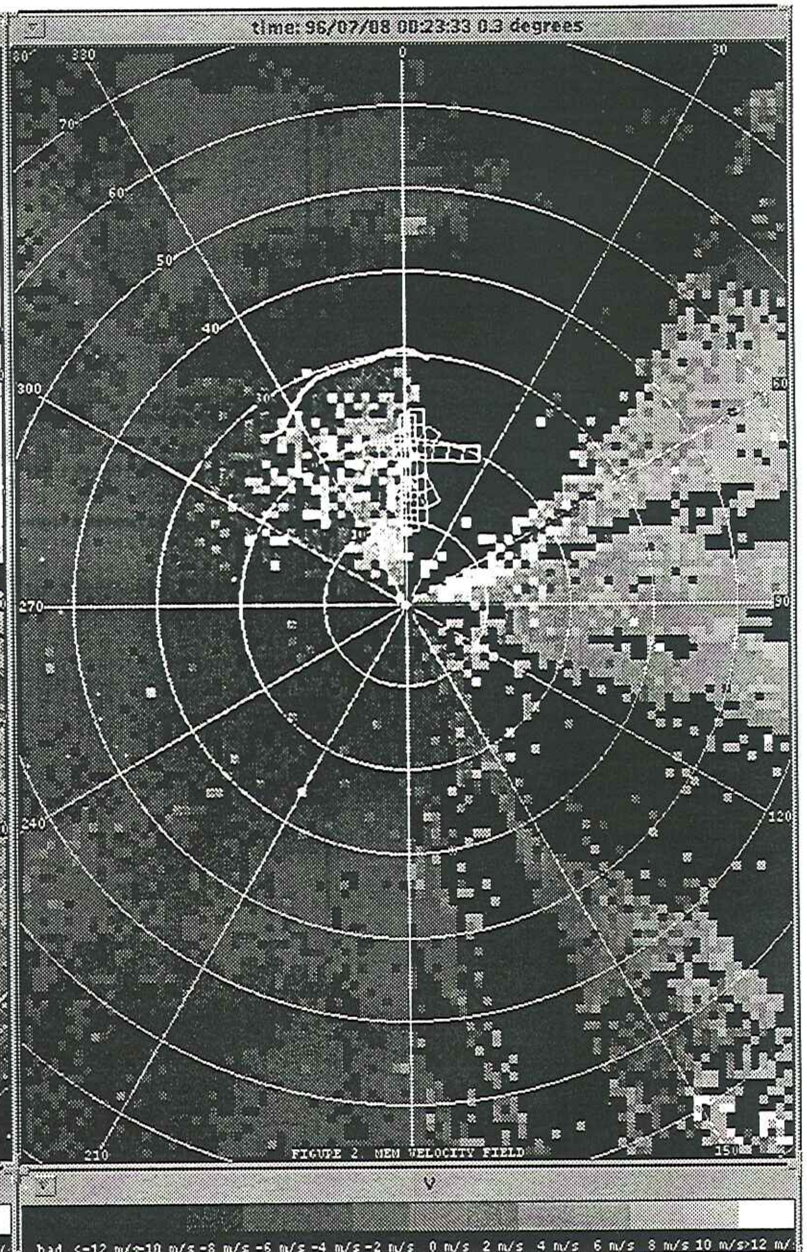

Figure 2. MEM TDWR velocity field showing gust front algorithm performance degradation due to range obscuration contamination on 08 July 1996.

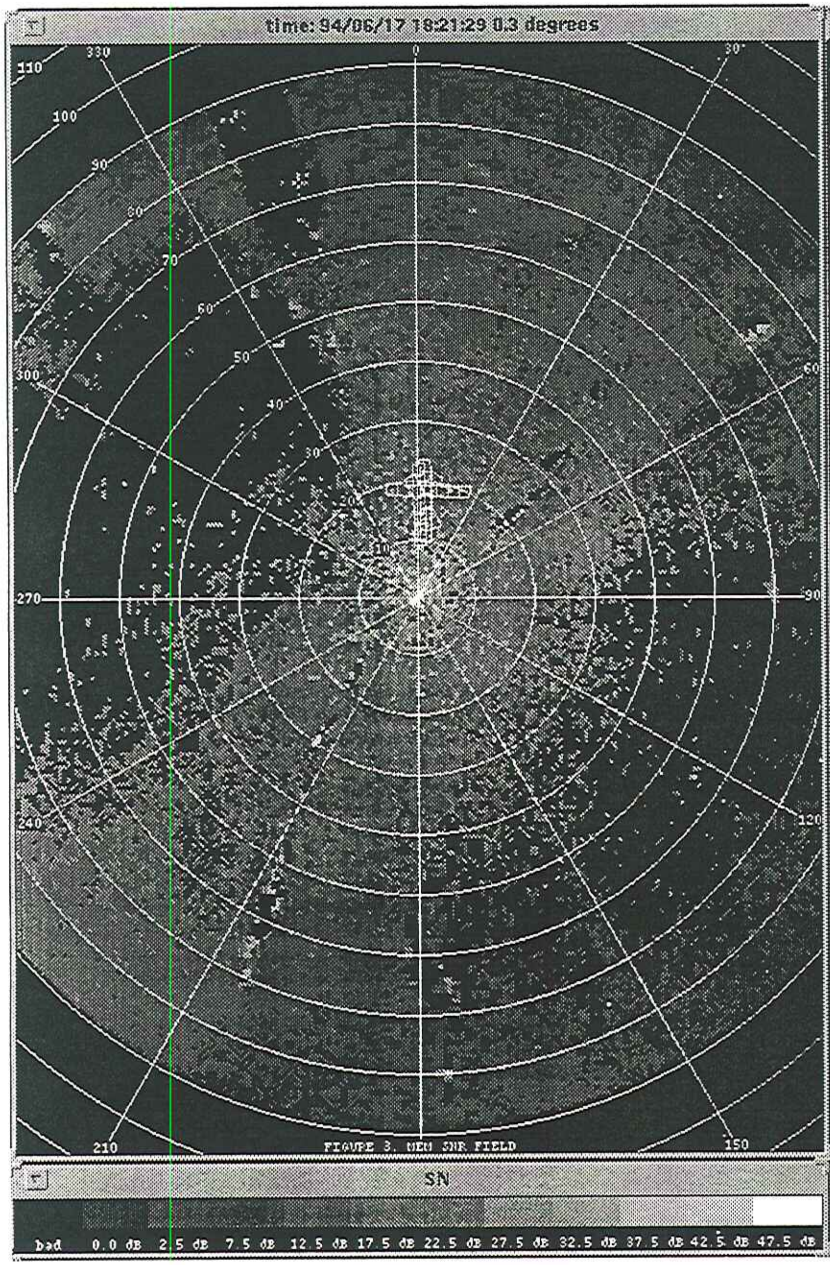

Figure 3. MEM TDWR SNR field on 17 June 1994 showing removal of clear-air returns on the 0.3 degree tilt.

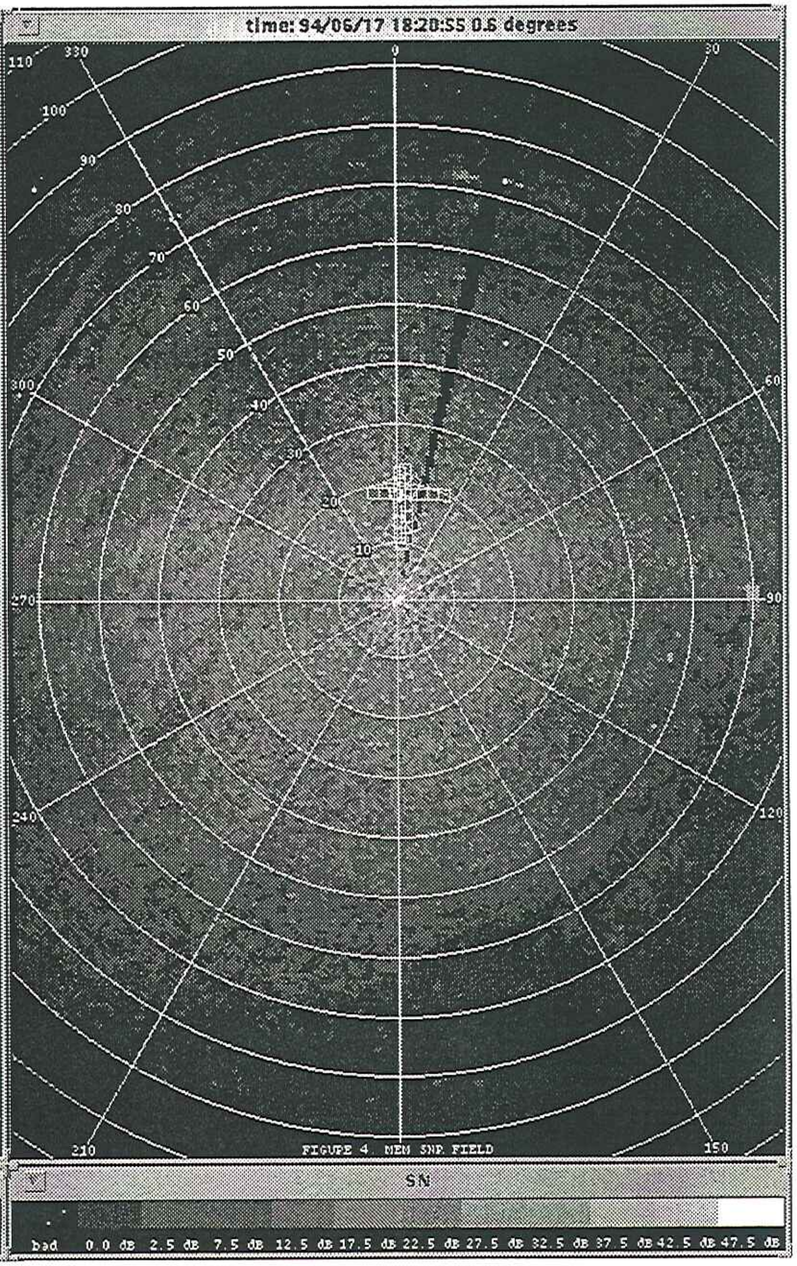

Figure 4. MEM TDWR SNR field on 17 June 1994 showing clear-air returns on the low PRF tilt.